Pflügers Arch – Eur J Physiol (1999) 437:812–822 

ORIGINAL ARTICLE

**Beate Illek · Albert W.-K. Tam · Horst Fischer**
**Terry E. Machen**

# Anion selectivity of apical membrane conductance of Calu 3 human airway epithelium

Received: 7 August 1998 / Received after revision: 2 December 1998 / Accepted: 3 December 1998

**Abstract** Anion selectivity of the cystic fibrosis conductance transmembrane conductance regulator (CFTR) and other channels and parallel pathways expressed endogenously in apical membranes of polarized Calu-3 epithelial monolayers was studied under control conditions and during cAMP stimulation. Basolateral membranes were eliminated using alpha-toxin. The cAMP-stimulated, gradient-driven currents had the sequence $Br \geq Cl \geq NO_3 > SCN > I \geq F >$ formate $> HCO_3 >$ acetate > propionate = butyrate = ATP = PPi = $PO_4 = SO_4 = 0$. Selectivity of parallel cAMP-independent pathway(s) was $Br > Cl = SCN = NO_3 > I >$ formate = $F > HCO_3 >$ acetate > propionate. SCN, I, F or formate blocked cAMP-stimulated, but not control, Cl currents. Anions >0.53 nm in diameter were impermeant, suggesting that the apical CFTR channel has a limiting diameter of 0.53 nm. The selectivity, blocking patterns and pore size of the cAMP-stimulated conductance pathway were very similar to those in previous reports in which CFTR was heterologously expressed in non-epithelial cells. Thus, CFTR appears to be the major apical anion conductance pathway in Calu-3 cells, and its conduction properties are independent of the expression system. CFTR in Calu-3 cells also conducts physiologically relevant anions, but not ATP, $PO_4$ or $SO_4$. A pathway parallel (probably a tight junction) showed a different selectivity than CFTR.

**Key words** Anion permeation · CFTR · Cystic fibrosis · Pore size · Tight junction

B. Illek · A.W.-K. Tam · H. Fischer · T.E. Machen (✉)
Department of Molecular and Cell Biology,
231 Life Science Addition, University of California at Berkeley,
Berkeley, CA 94720-3200, USA
e-mail: machen@socrates.berkeley.edu
Tel.: +1-510-6422983; Fax: +1-510-6436791

Beate Illek
Horst Fischer, Children's Hospital Oakland, Research Institute,
747 Fifty Second St., Oakland, CA 94609-1809, USA

## Introduction

The cystic fibrosis transmembrane conductance regulator (CFTR) Cl channel mediates cAMP-regulated Cl permeability in the apical membrane of a variety of Cl-transporting epithelia. CFTR is mutated in the genetic disease cystic fibrosis (CF), resulting in defective Cl transport across epithelia lining the airways, exocrine ducts and intestine [22]. CFTR functions primarily as a low-conductance Cl channel [1], although additional functions of the CFTR protein are under debate, e.g., as an ATP channel and also as a regulator of channels adjacent to the CFTR in the apical membrane of epithelial cells [20, 25, 26].

The selectivity of CFTR to different anions has been investigated extensively in patch-clamp measurements of permeability (from bi-ionic measurements of reversal potentials) or conductance (from slopes of *I*/*V* curves) from transfected cells or frog oocytes. The steady-state permeability for halides has largely been found to be $NO_3$(1.4)>Br(1.0–1.2)>Cl(1.0)>I(0.4–0.7)>F(0–0.3) [1, 2, 4, 5, 17, 18, 29, 33]. The low I permeability found in steady-state measurements is probably caused by the fact that, although I is quite permeant during initial channel exposure to the ion, I can enter the CFTR and block its own permeation as well as that of Cl [33]. There appear also to be differences in the permeability properties of CFTR depending on whether the anion permeates from the outside or the cytosolic side of the channel [17]. Less work has been done on physiologically relevant anions, but recent data showed that the permeability of CFTR expressed in Chinese hamster ovary (CHO) cells [17] or in frog oocytes [19] to polyatomic anions was formate (0.18) >$HCO_3$ (0.14) >acetate (0.09) [17]. The permeability of CFTR expressed in fibroblasts or MDCK cells to ATP has been reported to be either similar to that of Cl [20, 25] or zero [23]. The conductance of CFTR to various anions other than Cl has not been routinely measured, but it is generally agreed that the steady-state (as opposed to "initial") conductance sequence is Cl>I (e.g., [1, 18]), while Br has been reported to be both less conductive and more

conductive than Cl, e.g., Br/Cl=0.6 –0.65 [12, 18] or Br/Cl=1.3 [1].

Measurements of CFTR's permeability in polarized epithelial cells in confluent monolayers have been limited to reversal potential measurements from T84 cells, which gave $NO_3$(1.4)>Br(1.2–1.3)>Cl(1.0)>I(0.6) [1, 2]. This sequence largely agrees with patch-clamp measurements of CFTR's permeability when expressed in frog oocytes, and a variety of fibroblast cell lines [1, 17, 18, 33]. In contrast, patch-clamp studies of CFTR in single pancreatic duct cells showed the permeability sequence to be $NO_3$(1.7–3.0)>Br=Cl=I(1.0) [7, 8]. Also, $HCO_3$ was permeant through CFTR in pancreatic ($HCO_3$/Cl =0.11–0.25) [8], 3T3 ($HCO_3$/Cl=0.25) [21], Calu 3($HCO_3$/Cl=0.15) [14] and CHO ($HCO_3$/Cl=0.14) [17] cells, but not through CFTR in sweat duct cells [23]. CFTR has been reported to conduct ATP at rates that can be measured electrophysiologically [25, 26], and also to control the permeation of ATP through associated channels [20]. In contrast, no detectable ATP conductance was found in freshly isolated sweat duct epithelial cells, single Calu-3 cells, or CHO cells recombinantly expressing CFTR and CFTR reconstituted into planar lipid bilayers [9, 15, 23]. Some of these differences may have arisen from the fact that studies of CFTR selectivity in T84 cells have been done on permeabilized cells in intact monolayers (where normal channel orientation will have been maintained), while patch-clamp studies have been conducted on CFTR expressed in nonepithelial cells or on single, isolated epithelial cells (where distribution and attachments within the cell will have been abnormal or disrupted). Permeation of other physiologically relevant polyatomic anions (e.g., acetate, pyrophosphate, phosphate, sulfate, fatty acids) and potential interactions among Cl and such permeant ions have not been reported for CFTR expressed in polarized monolayers.

Given the relative lack of data on CFTR's selectivity in native epithelial cells (and none in airway cells at 37°C) and the apparent variability in permeability and conductance properties of CFTR depending on the cell type in which it was expressed, it seemed important to measure the selectivity of CFTR expressed in its physiological state, i.e., in the apical membrane of an airway epithelium at 37°C. Since single-channel recordings might underestimate permeability ratios when the test ion inhibits gating or has very low permeability, we measured cAMP-stimulated gradient-driven currents for each test anion in the absence of Cl on the opposite side. The purposes of this study were to:

1. Compare the conductance sequence for a variety of anions that have been studied previously for CFTR expressed recombinantly in single cells. These data could then be used to compare the pore size of the CFTR expressed in a polarized fashion in the airway epithelial cell in the intact monolayer to those reported in heterologous expression systems and studied at room temperature.
2. Determine interactions of other anions on Cl permeation through CFTR.
3. Determine anion selective pathways in parallel to CFTR.

We used human Calu-3 cells which have been shown to have characteristics of serous glands (the major site of Cl secretion in the airways) and to express large amounts of CFTR in the apical cell membrane [11, 27], whereas a Ca-activated Cl conductance is absent in the apical membrane [27]. In a recent study we used Calu 3 monolayers in which the basolateral membrane had been permeabilized with *Staphylococcus aureus* α-toxin to show that apical membrane Cl currents in Calu 3 cells are activated by basolateral addition of cAMP and ATP, and further stimulated by genistein and bromotetramisole, and blocked by glibenclamide and diphenylamine-2-carboxylate (DPC) but not 4,4′-diisothiocyanatostilbene-2,2′-disulfonic acid (DIDS) and 4,4′-dinitrostilbene-2,2′-disulfonic acid (DNDS) [14], all of which are hallmarks of CFTR activity. This approach allowed us in the present work to determine the anion selectivity of the apical cAMP-stimulated Cl conductance, and eliminated possible contributions made by other Cl conductances that may be found in either the apical or the basolateral membrane of undifferentiated, isolated cells. For example, the ORCC Cl channel with a selectivity of I>Cl is a dominant current-carrying channel in isolated colonic T84 cells [10] and is also present in single Calu-3 cells [11]. However, when T84 cells are grown as confluent monolayers, CFTR is the dominant current-carrying channel in the apical membrane with a steady-state conductance and permeability selectivity Cl>I [1, 2].

## Materials and methods

### Cell culture

Calu-3 cells, a human airway cell line of pulmonary adenocarcinoma origin, were kindly provided by Dr. J.H. Widdicombe (Children's Hospital Oakland, Calif., USA). Calu-3 cells form a polarized monolayer and endogenously express CFTR in the apical cell membrane [27]. Standard cell-culture techniques were used as described [14]. Cells were seeded directly onto permeable filters (0.45 μm pore size, 12 mm diameter; Falcon, Becton Dickinson, Franklin Lakes, N.J., USA). After plating, the transepithelial resistances were monitored using an epithelial voltohm-meter (EVOM; World Precision Instruments). Cells grown as monolayers were used between 5–14 days and transepithelial resistances ($R_T$) of intact monolayers ranged from 0.8–2.0 kΩ.cm$^2$.

### Electrical measurements

Short-circuit current measurements were done exactly as described elsewhere [14]. Briefly, Calu-3 monolayers grown on filters were carefully cut from the plastic insert, mounted in a modified Ussing chamber, short-circuited, and the resulting short-circuit current was recorded. Voltage pulses of 2 mV (every 20 s) were used to determine $R_T$ and transepithelial conductance ($G_T$) using Ohm's law. Negative currents were defined as anion movement from mucosa to serosa. Voltage was referenced to the mucosal side. The relative conductance sequence for a series of anions was determined from the cAMP-stimulated portion of currents generated by equivalent transepithelial ionic gradients. Both chamber compartments were separately and continuously perfused

**Table 1** Effect of apparent equilibrium potentials on the current ratio sequence of permeable anions. Values are means ±SE. (*n* Number of experiments.) The apparent equilibrium potential ($\Delta E_{ion}$) was calculated according to Ohm's law ($\Delta I/\Delta G$) from the cAMP-stimulated portion of apical currents ($\Delta I$) and corresponding conductance changes ($\Delta G$) for each permeable anion. $c_a/c_b$ is the apparent concentration ratio resulting from the applied gradient (135:0 mM), see Materials and methods. The factor was calculated from the apparent concentration ratio relative to Cl from paired experiments. $ratio_{corr}$ is the corrected ratio obtained from corrected cAMP-stimulated currents relative to Cl ($corr\Delta I_{cAMP,X}/corr\Delta I_{cAMP,Cl}$)

| Mucosal anion | $E_{ion}$ (mV) | $c_a/c_b$ | Factor | $Ratio_{corr}$ | *n* |
|---|---|---|---|---|---|
| Bromide | –20.5±1.5 | 2.11±0.13 | 1.04±0.03 | 1.04±0.04 | (6) |
| Chloride | –22.3±1.1 | 2.42±0.12 | 1.0 | 1.0 | (31) |
| Nitrate | –24.5±1.6 | 2.58±0.16 | 0.90±0.03 | 0.97±0.07 | (5) |
| Thiocyanate | –22.0±0.8 | 2.33±0.07 | 0.99±0.11 | 0.63±0.05 | (3) |
| Iodide | –18.7±2.7 | 2.10±0.21 | 1.04±0.06 | 0.59±0.03 | (5) |
| Fluoride | –15.0±2.1 | 1.80±0.14 | 1.20±0.08 | 0.52±0.08 | (5) |
| Formate | –15.0±2.8 | 1.81±0.19 | 1.89±0.19 | 0.38±0.11 | (4) |
| $HCO_3$ | –24.9±2.7 | 2.86±0.41 | 0.99±0.17 | 0.24±0.05 | (16) |
| Acetate | –13.4±2.6 | 1.67±0.20 | 1.57±0.12 | 0.12±0.03 | (6) |

at 37°C. Constant perfusion was used to reduce build-up of the test ion in the serosal solution and/or cytosol which would diminish the applied gradient.

### Permeabilization of the basolateral membrane

The basolateral membrane of Calu-3 monolayers was permeabilized by using the pore-forming agent *Staphylococcus aureus* alpha-toxin (Calbiochem, La Jolla, Calif., USA). α-Toxin forms transmembrane pores (1.14 nm in diameter) and induces the transport of macromolecules up to 2 kDa in size [30]. Permeabilization of the basolateral membrane allowed us to investigate the apical membrane in isolation. Before measurements, the serosal side of the monolayers was incubated with 250 U/ml α-toxin for 30 min at 37°C. In a previous study of α-toxin permeabilized Calu-3 cells, we identified CFTR as the current carrier under these conditions without any contribution of basolateral membrane transporters [14]. Furthermore, involvement of a Ca-activated Cl conductance during our measurements was not possible since there is no significant Ca-activated Cl conductance in the apical membrane of Calu-3 cells [27].

### Solutions

The serosal reference solution contained (in mM): 135 Na-gluconate, 0.1 $CaCl_2$, 2.4 $K_2HPO_4$, 0.6 $KH_2PO_4$, 20 HEPES, 10 glucose, and 5 MgATP. To determine the relative conduction of anions, the main anion (*X*) was replaced by an equimolar amount of the respective Na salt on the mucosal side. The mucosal standard solution contained (in mM): 135 Na*X*, 1.2 $MgSO_4$, 1.2 $CaSO_4$, 2.4 $K_2HPO_4$, 0.6 $KH_2PO_4$, 20 HEPES and 10 glucose. The following anions were used: Cl, Br, I, F, $HCO_3$, $NO_3$, SCN, formate, acetate, propionate, butyrate, $SO_4$, $PO_4$, pyrophosphate (PPi), and ATP. Solutions were prepared so that there were no gradients other than for the test ion. $SO_4$ solution was prepared from 135 mM $NaHSO_4$. Phosphate solution contained 135 mM $NaH_2PO_4$. PPi solution contained 33.75 mM $Na_4P_2O_7$ and 101.25 mM mannitol. ATP solution contained 67.5 mM $Na_2ATP$ and 67.5 mM TrisATP (Sigma, St. Louis, Mo., USA). At pH 7.4 these polyvalent anions carry average charges of –1.6 ($PO_4$), –2.96 (PPi), –3.88 (ATP), respectively. In order to account for the differences in the charge and concentration of polyvalent anions in solutions used, the resulting gradient-driven currents can be corrected by the factor: (standard concentration)/(employed concentration × average valence). However, since none of the polyvalent anions in this report caused any detectable currents, no corrections of measured currents were performed. cAMP (100 µM, Na salt, Sigma) was added to the serosal solution to stimulate CFTR activity. All solutions were adjusted to pH 7.4 with *N*-methyl-d-glucamine.

### Data analysis

In the presence of a gradient for test anions (*X*, mucosal; gluconate, serosal) the difference between the baseline current ($I_{ctrl}$) and the cAMP-stimulated current ($I_{cAMP}$) was used as a measure of conductive current flow ($\Delta I=I_{cAMP}-I_{ctrl}$) induced by the anion gradient across the CFTR-mediated conductance pathway. In our experiments the concentration of test ions was 135 mM in the apical solution, while the basolateral concentration was 0 mM (0.2 mM for Cl). This experimental procedure resulted in the measurement of the conductance for most ion species at an anion concentration gradient of 135:0 mM clamped to 0 mV. During exposure of the apical side to the different test ions, some ions permeated and accumulated in the unstirred layer formed by the cells and solution closely adjacent to the surface. This accumulation of the test ion reduced the gradient to some value less than 135:0 mM (0.2 for Cl). We corrected for this effect using the following procedure. Since transepithelial voltage (*V*) was clamped to 0 mV during these experiments, the apparent equilibrium potential ($E_{ion}$) calculated as $E_{ion}=\Delta I_{cAMP}/\Delta G_{cAMP}$ should have been equal to the value of the chemical driving force for the test ion across the epithelium. As summarized in Table 1, $E_{ion}$ for all the ions were between –13.4 mV ($E_{acetate}$) and –24.9 mV ($E_{HCO3}$). Using the Nernst equation, $E_{ion}$ values were converted to the ratio of concentrations on the apical versus the cell-basolateral surface during the exposure to the test ion in the apical solution. For example, $E_{Cl}$=–22.3 mV =–60×log ($[Cl]_{apical}/[Cl]_{basal}$]) resulted in an apparent concentration ratio of $[Cl]_{apical}/[Cl]_{basal}$=2.4. Similar calculations were performed for all the other ions which showed that the gradient varied between 2.86 ($HCO_3$) and 1.67 (acetate). The implication of these calculations was that the ionic gradients were all similar, but were not exactly equal. When comparing currents from all the test ions to those of Cl, $\Delta I_{cAMP,X}$ will have been overestimated when the test ion gradient was larger than that for Cl (2.4), while for ions with smaller gradients $\Delta I_{cAMP,X}$ will have been underestimated. We corrected for this effect as follows: $\Delta I_{cAMP,Xcorrected}=\Delta I_{cAMP,X}\times 2.4/([X]_{apical}/[X]_{basal})$. As shown in Table 1, these corrections affected the calculated current ratios for $NO_3$, F, formate and acetate, whereas the permeation sequence was only affected for $NO_3$ [uncorrected: $NO_3$ (1.09)>Cl; corrected: Cl>$NO_3$ (0.97)]. We show corrected selectivity ratios in Figs. 5C and 7.

In addition, $I_{cAMP}$ might have also been affected by the cytosolic presence of gluconate and HEPES buffer in our solution, which have been shown to block CFTR [16, 33]. However, all test anions were probably affected to a similar extent by these factors. Under unstimulated conditions (in the absence of cAMP), parallel currents ($I_{para}$) were calculated for each anion from $I_{ctrl,X}-I_{ctrl,gluconate}$.

Data are given as means ±SE; *n* refers to the number of monolayers examined. Statistical analysis was performed by paired or unpaired Student's *t*-tests. Probabilities of $P<0.05$ were considered

significant. The dimensions of the test anions were estimated using a computer program (Molecular Modeling Pro, WindowChem Software, Fairfield, Calif., USA). Polyatomic anions were modeled as rectangular prisms, and the largest width rectangular to the maximal length of the molecule was used as the effective diameter of the anion.

## Results

### Conductance of halides across cAMP-stimulated and unstimulated Calu-3 cells

Monolayers were exposed to α-toxin on the basolateral side as described in Materials and methods to remove the basolateral membrane as a functional barrier and yield a single membrane preparation. Initially all permeabilized monolayers were bathed in symmetrical gluconate Ringers. Currents were close to zero and unchanged by addition of cAMP (Table 2, $P>0.05$). Figure 1A,B shows currents generated by gradients of Br, Cl, I and F in the presence ($I_{cAMP}$) and absence ($I_{ctrl}$) of cAMP, respectively. In the continued presence of cAMP, exchanging mucosal gluconate for Br induced an average $I_{cAMP}$ of –181.7±13.2 μA/cm² ($n$=7); further exchange with Cl decreased $I_{cAMP}$ to –161.8±6.1 μA/cm² ($n$=42). Exchanging Cl for I typically induced a transient response of $I_{cAMP}$ that stabilized at –113.7±6.2 μA/cm² ($n$=5). Replacement of I by F further decreased $I_{cAMP}$ to –81.2±5.6 μA/cm² ($n$=5).

Both F and I elicited transient changes of $I_{cAMP}$ that were different during initial versus steady-state conditions, indicating that these ions interact in a complicated fashion with the channel, perhaps due to multi-ion pore behavior [32, 33]. When solutions were exchanged in our experiments, there was a brief period when the two ion species mixed, which, in a multi-ion pore, can lead to a current block. In addition, I has been reported to permeate and block CFTR from the cytosolic side [33]. The observed transients of transepithelial current responses may have been caused by similar types of effects.

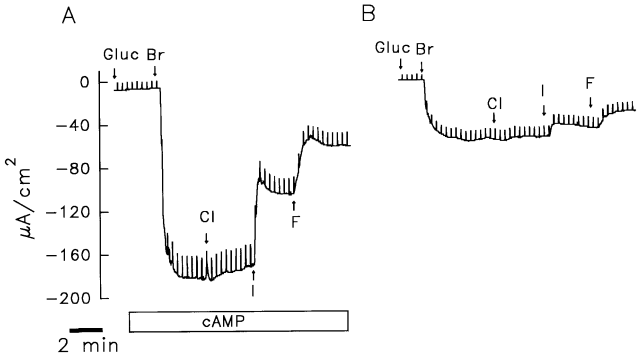


**Fig. 1A, B** Halide selectivity. Effects of Br, Cl, I and F on apical currents in basolaterally α-toxin-permeabilized Calu-3 monolayers. Currents were measured in the presence of a mucosal-to-serosal gradient for Br, Cl, I or F (135 mM); the serosal side faced 135 mM Na-gluconate Ringer. **A** When gluconate was the principle anion on the mucosal side, serosal addition of 100 μM cAMP had no effect. Exchange of mucosal gluconate for Br resulted in a rapid current increase across the apical membrane. Subsequent exchange of Br with Cl, I and F elicited step-wise reductions in current. **B** Unstimulated tissues showed similar current selectivity for halides, but currents were smaller. Differences between basal and cAMP-stimulated currents ($I_{cAMP}$)were used to calculate selectivity ratios for $I_{cAMP}$

We also tested the effects of anion substitution in unstimulated monolayers, i.e., effects on paracellular and transcellular anion conductive pathways parallel to CFTR. $I_{ctrl}$ were small compared to $I_{cAMP}$. Gradient-driven control currents displayed the same halide sequence (Fig. 1B) as across cAMP-stimulated monolayers; however, we will show below that SCN and propionate are conducted through these parallel conductances with a different selectivity compared with CFTR. In addition, we have previously shown that $I_{ctrl}$ is not blocked by the CFTR blocker DPC [14], indicating that $I_{ctrl}$ is not significantly mediated by CFTR, but reflects conductive pathways that lie parallel to CFTR (most likely paracellular/tight junctions).

**Table 2** Effect of mucosal anions on apical currents of α-toxin permeabilized Calu-3 monolayers. Values are means ±SE; ($n$ Number of experiments.) Unstimulated ($I_{ctrl}$) and cAMP-stimulated ($I_{cAMP}$) currents across the apical membrane and corresponding transepithelial resistances ($R_T$) of α-toxin-permeabilized Calu-3 monolayers were measured by applying a mucosal-to-serosal anion gradient before and after serosal addition of 100 μM cAMP. On the mucosal side 135 mM Na-gluconate was equimolarily replaced by the tested anion. The serosal side contained Na-gluconate Ringer + 5 mM MgATP and 0.1 mM $CaCl_2$ in all experiments

| Mucosal anion | Before cAMP | | | cAMP-stimulated | | |
|---|---|---|---|---|---|---|
| | $I_{ctrl}$ (μA/cm²) | $R_T$ (Ω · cm²) | $n$ | $I_{cAMP}$ (μA/cm²) | $R_T$ (Ω · cm²) | $n$ |
| Gluconate | –2.5±0.4 | 569.4±48.4 | (66) | –3.2±0.9 | 672.4±134.5 | (13) |
| Cl | –50.8±3.4 | 261.0±17.1 | (50) | –161.8±6.1* | 103.1±9.5* | (42) |
| Bromide | –64.6±4.5 | 213.0±17.6 | (7) | –181.7±13.2* | 96.4±4.1* | (7) |
| Iodide | –45.3±4.6 | 235.0±35.1 | (6) | –113.7±6.2* | 132.3±10.8* | (5) |
| Fluoride | –28.8±3.2 | 268.2±49.1 | (6) | –81.2±5.6* | 132.5±11.4* | (5) |
| Nitrate | –44.0±14.4 | 233.0±49.0 | (5) | –168.2±18.7* | 113.6±18.4* | (9) |
| Thiocyanate | –53.9±2.3 | 143.0±7.0 | (3) | –128.0±13.2 | 97.3±7.9* | (3) |
| $HCO_3$ | –10.1±1.4 | 632.0±91.1 | (20) | –31.7±3.5* | 413.0±38.1* | (20) |
| ATP | 1.2±1.0 | 495.8±66.8 | (5) | 0.3±2.6 | 461.2±60.5 | (5) |
| Phosphate | 2.1±1.3 | 622.5±57.5 | (2) | 3.0±2.3 | 537.5±27.5 | (2) |
| PPi | 3.3±2.0 | 431.7±70.0 | (4) | 4.3±3.8 | 397.0±55.6 | (4) |
| Sulfate | –5.7±1.4 | 460.0±115.0 | (3) | –6.3±1.7 | 477.7±33.8 | (3) |
| Formate | –25.1±3.1 | 307.8±41.7 | (5) | –68.2±18.1* | 170.2±39.7* | (5) |
| Acetate | –7.3±1.7 | 436.0±31.0 | (6) | –12.8±1.7* | 390.5±41.7 | (7) |
| Propionate | –6.1±1.6 | 212.5±82.9 | (3) | –6.1±1.6 | 212.5±82.9 | (3) |
| Butyrate | –3.6±1.6 | 358.2±46.6 | (6) | –4.4±2.0 | 297.7±42.7 | (6) |

* Significantly different from before cAMP ($P<0.05$, unpaired $t$-test)

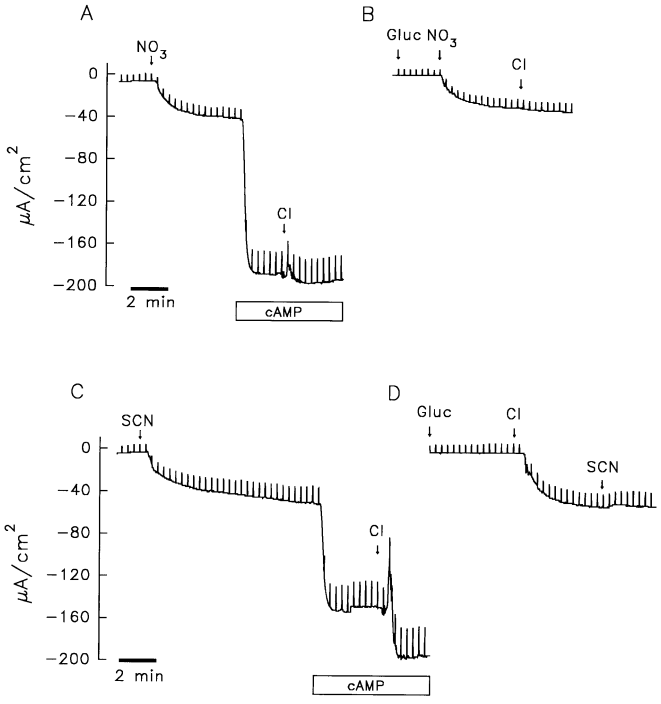


**Fig. 2A–D** Effects of the polyatomic anions $NO_3$ and SCN. **A** Replacement of gluconate with $NO_3$ induced currents across the apical membrane that were stimulated by serosal addition of cAMP (100 μM). Exchange of $NO_3$ for Cl slightly increased currents. **B** Control, gradient-driven currents were not different for $NO_3$ or Cl. **C** SCN currents were stimulated by serosal cAMP. Exchange of SCN for Cl resulted in a rapid, transient decrease of current followed by a sustained elevated current. **D** In the absence of cAMP, SCN currents were slightly smaller than Cl currents

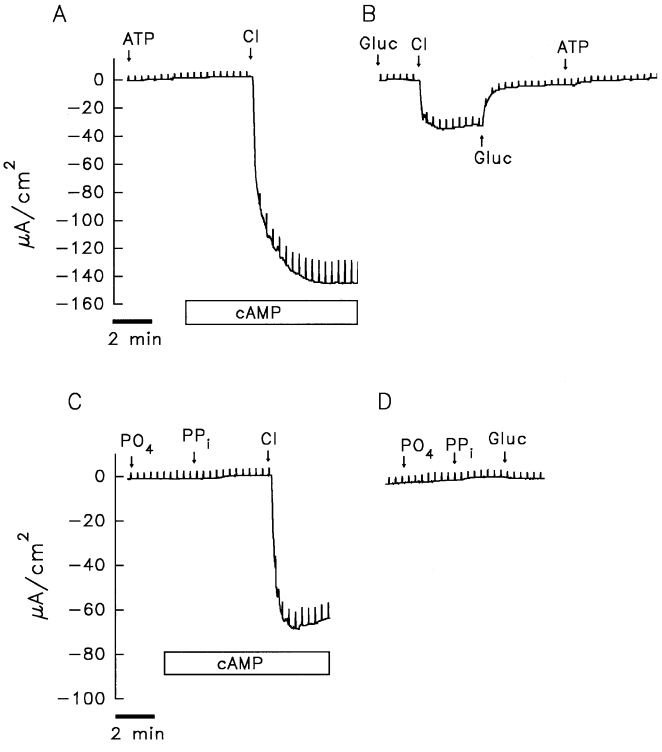


**Fig. 3A–D** Lack of effect of cAMP when ATP, phosphate (*PO4*) and pyrophosphate (*PPi*) are the principal mucosal anions. **A** No currents were measured under control or cAMP-stimulated conditions when ATP was the principle anion on the mucosal side. Exchange of apical ATP for Cl restored current. **B** Unstimulated control shows reversible increase of control current after Cl replacement; current was unaltered when gluconate was replaced by ATP. **C** Lack of stimulation of apical currents by cAMP when $PO_4$ or PPi were the main mucosal anions. **D** Unstimulated control. Baseline currents were not affected by $PO_4$ or PPi

When $I_{cAMP}$ was corrected for $I_{ctrl}$, the cAMP-stimulated portion of $I_{cAMP}$ ($\Delta I$) was on average –113.8±14.9 μA/cm² (*n*=6) for Br, –104.2±8.9 μA/cm² (*n*=42) for Cl, –68.4±11.4 μA/cm² (*n*=5) for I, and –49.5±8.3 μA/cm² (*n*=5) for F. The relationship between the $\Delta I$ of the test anion and that of Cl was obtained from paired data and yielded an average selectivity ratio ($\Delta I_X/\Delta I_{Cl}$) of cAMP-stimulated, apical currents of 1.02±0.3 (*n*=6) for Br, >1.0 for Cl, >0.57±0.02 (*n*=5) for I and >0.43±0.06 (*n*=5) for F. In parallel, the cAMP-stimulated transepithelial conductance change ($\Delta G$) was 6.0±0.6 mS/cm² for Br, 4.9±0.5 mS/cm² for Cl, 3.7±0.4 mS/cm² for I and 3.4±0.5 mS/cm² for F.

## Permeation of polyatomic anions: $NO_3$, SCN and $HCO_3$

Imposing the mucosal-to-serosal $NO_3$ gradient increased $I_{ctrl}$ to –44.0±14.4 μA/cm², and cAMP further stimulated currents to –141.0±20.0 μA/cm² (*n*=27) (Fig. 2A). In nine paired experiments replacing $NO_3$ by Cl had no significant effect on $\Delta I$ (–96.8±18.0 μA/cm² versus –94.4±21.8 μA/cm² for $NO_3$ and Cl, respectively) and $\Delta G$ ($NO_3$: 4.0±0.8 mS/cm², Cl: 4.1±0.9 mS/cm²), indicating that $NO_3$ and Cl are equally conducted through CFTR. As shown in Fig. 2B, $NO_3$ and Cl elicited similar currents across the unstimulated monolayers.

When cells were exposed to an SCN gradient, the average $I_{ctrl}$ was –53.9±2.3 μA/cm², and $I_{cAMP}$ was stimulated to –128.0±13.2 μA/cm² (*n*=3), yielding a $\Delta I_{SCN}$ of –74.1±14.8 μA/cm² (see Fig. 2C, D). The corresponding $\Delta G$ was 3.4±0.7 mS/cm². Exchanging SCN for Cl caused an initial rapid spike in $I_{cAMP}$ followed by a fast recovery to a level significantly increased when compared to that measured in the presence of SCN. In contrast, $I_{ctrl}$ was similar in the presence of SCN or Cl (Fig. 2D, Table 2).

In a previous study we showed that CFTR mediates $HCO_3$ currents across the apical membrane of Calu-3 cells (see Table 1 and Figs. 5–8 from [14]). For comparison, additional data obtained with $HCO_3$ were combined in this study (Table 2). In 20 paired experiments $\Delta I$ was –21.3±2.9 μA/cm² for $HCO_3$ and –126.7±12.1 μA/cm² for Cl. The corresponding $\Delta G$ was 1.1±0.1 mS/cm². Taking data from paired experiments yielded a current ratio sequence ($\Delta I_X/\Delta I_{Cl}$) of 1.09±0.10 (*n*=5) for $NO_3$, >0.64±0.02 (*n*=3) for SCN, and >0.21±0.04 (*n*=20) for $HCO_3$.

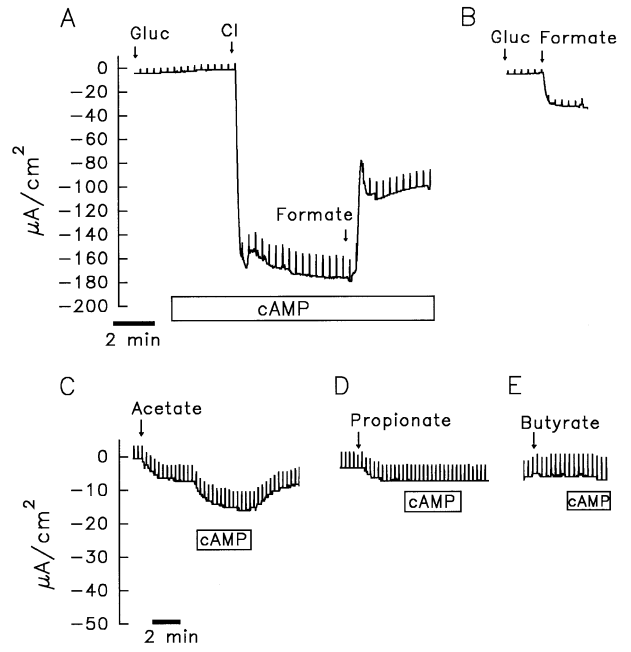


**Fig. 4A–E** Conduction of short-chain fatty acids. **A** Stimulation of apical currents in the presence of Cl, but not gluconate. Further exchange of formate with Cl decreased currents biphasically, and formate currents leveled off at a new, stable, stimulated level. **B** Unstimulated control. Exchanging formate for gluconate increased currents that were less than those observed under stimulated conditions. **C** Effect of acetate on currents in unstimulated cells and further stimulation by cAMP. **D** Effect of propionate replacement on unstimulated current and lack of stimulation by cAMP, indicating that propionate is not conducted through CFTR. **E** Butyrate replacement has no significant effect on currents of unstimulated cells. Butyrate permeability was not stimulated by cAMP

## Lack of permeation of the polyvalent anions ATP, $PO_4$, PPi, and sulfate

Since there is controversy over CFTR-mediated permeation of ATP [20, 24, 25, 26], we tested the cAMP-dependent stimulation of apical current in the presence of an ATP gradient in Calu-3 monolayers. In addition, we tested $PO_4$ and PPi, which, as parts of the ATP molecule, might show size-governed conductances. $I_{ctrl}$ in the presence of an ATP gradient (135:5 mM) was close to zero (1.2±1.0 μA/cm², $n$=5), and no measurable current was stimulated by cAMP ($\Delta I$=0.12±0.17 μA/cm², $n$=5, Fig. 3A, B). Figure 3C and D illustrate that $PO_4$ (135:0 mM) and PPi (33.75:0 mM) also had no effect on $I_{ctrl}$ and $I_{cAMP}$ (see Table 2). The respective $\Delta I$ values (0.10±1.08 μA/cm², $n$=2 and 0.90±2.08 μA/cm², $n$=4) were not different from zero. These results demonstrate that ATP, $PO_4$ and PPi are not conducted from the mucosal to the serosal side by an electrogenic mechanism through CFTR. $SO_4$ ($\Delta I$=0.60±0.32 μA/cm², $n$=3) was similarly not conducted (Table 2). Therefore, none of these multivalent anions generated measurable currents across CFTR in apical membranes of Calu 3 cells.

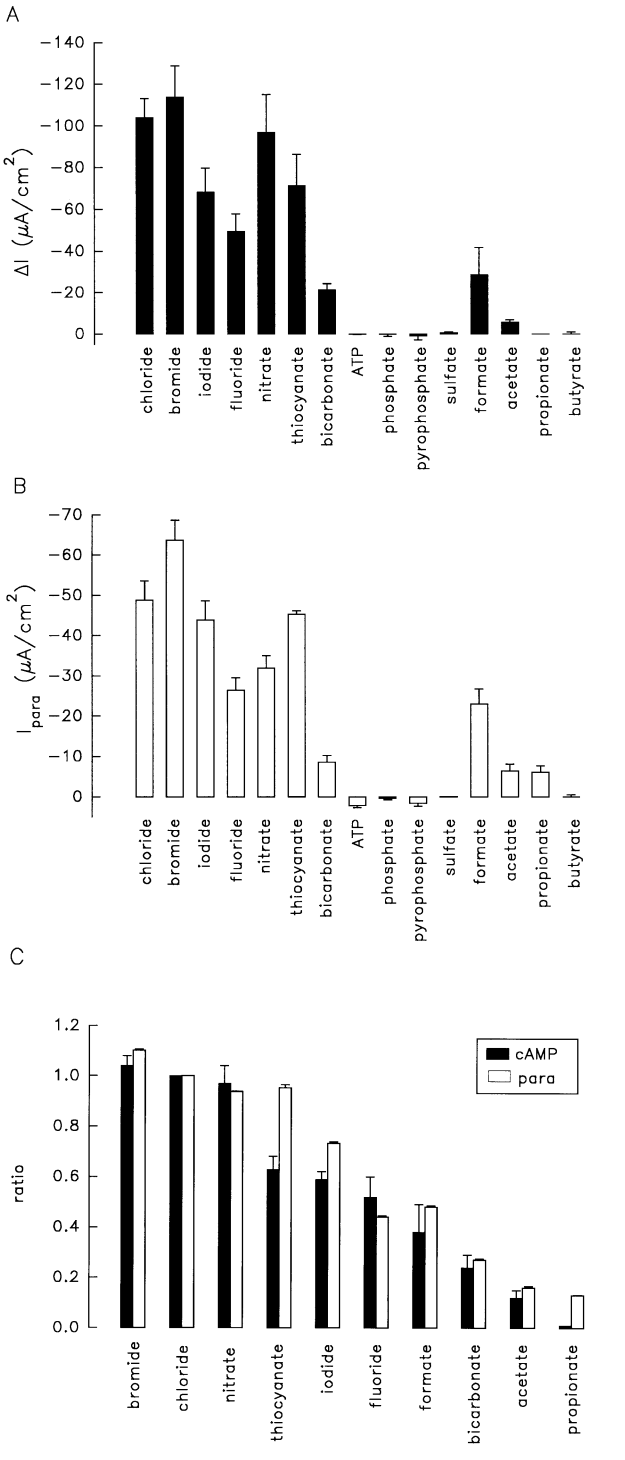


**Fig. 5** **A** Summary of average currents through CFTR ($\Delta I_{cAMP}$) for all tested anions. $\Delta I_{cAMP}$ was affected by chloride, fluoride, bromide, iodide, nitrate, thiocyanate, bicarbonate, formate and acetate. **B** Summary of average paracellular currents ($I_{para}$) for all anions. **C** Selectivity ratio sequences ($I_X/I_{Cl}$) of CFTR-mediated currents in the presence of cAMP (*filled bars*; corrected ratios, see Table 1) and parallel conductances in the absence of cAMP (*open bars*) for permeable anions. $I_{para}$ was affected to a different extent by SCN. $I_{para}$ was affected by propionate, whereas $\Delta I_{cAMP}$ was not affected by this anion

### Permeation of short-chain fatty acids: formate, acetate, propionate and butyrate

Short-chain fatty acids (SCFA) are transported across the large intestine [35], which expresses high levels of CFTR. We tested the conductance of SCFA across CFTR for their physiological importance and for their increasing molecular size while carrying a single negative charge, which appeared to be favored by CFTR. After stimulation with cAMP, formate-gradient driven current was $I_{cAMP}$=–68.2±18.1 μA/cm² (Fig. 4A), and $I_{ctrl}$ was –25.1±3.1 μA/cm² (Fig. 4B), yielding a $\Delta I$ of –28.6±13.0 μA/cm² ($n$=5). The corresponding $\Delta G_T$ was 1.8±0.7 mS/cm². Acetate gradients generated an $I_{cAMP}$ of –13.7±1.7 μA/cm² and an $I_{ctrl}$ of –8.0±1.8, yielding a $\Delta I$ of –5.7±1.1 μA/cm² ($n$=6) (Fig. 4C), and the corresponding $\Delta G_T$ was 0.4±0.2 mS/cm². A propionate gradient elicited a detectable $I_{ctrl}$ but no $I_{cAMP}$ ($\Delta I$=0.0 μA/cm², $n$=3) (Fig. 4D). Butyrate gradients had a minor effect on $I_{ctrl}$ and no effect on $I_{cAMP}$ ($\Delta I$=0.89±0.82 μA/cm², $n$=5, see Fig. 4E). The selectivity ratios sequence for the SCFA (relative to Cl from paired experiments) across CFTR was formate (0.23±0.12, $n$=4) >acetate (0.08±0.02, $n$=6) >propionate (0.0, $n$=3) =butyrate (0.0, $n$=5).

### cAMP-stimulated and paracellular current selectivity sequence

Figure 5A illustrates the cAMP-stimulated current changes ($\Delta I$) for each anion. Current changes smaller than 2 μA/cm² (corresponding to 2% of $I_{cAMP}$ yielded by Cl) were difficult to discriminate from baseline drift. Therefore, the anions ATP, $PO_4$, PPi, $SO_4$, propionate and butyrate were not (or less than 2%) conducted by CFTR. Figure 5B illustrates average paracellular currents ($I_{para}$ as calculated from average $I_{ctrl,X}$–$I_{ctrl,\ gluconate}$) for each anion. Figure 5C compares the selectivity sequences of cAMP-stimulated and paracellular current ratios compared to Cl. The selectivity sequence for the cAMP-stimulated portion ($\Delta I_X/\Delta I_{Cl}$) as calculated from correction factors listed in Table 1 was Br (1.04±0.04) ≥Cl(1.0)≥$NO_3$(0.97±0.07)>SCN(0.63±0.05)≥I0.59±0.03) ≥F(0.52±0.08)>formate (0.38±0.11)>$HCO_3$(0.24±0.05) >acetate (0.12±0.03). The selectivity sequence for anion currents in parallel to CFTR ($I_{para}$) (sequenced by ratio $I_{para,X}/I_{para,Cl}$) was Br (1.10±0.05, $n$=7)>Cl(1.0)≥SCN (0.95±0.12, $n$=3)≥$NO_3$(0.94±0.02, $n$=5)>I(0.73±0.07, $n$=6) >formate (0.48±0.05, $n$=4)≥F (0.44±0.05, $n$=6)>$HCO_3$ (0.27±0.03, $n$=8)>acetate (0.16±0.06, $n$=5)≥propionate (0.13±0.02, $n$=2). Relatively smaller current ratios through CFTR compared to $I_{para}$ (0.64 versus 0.95) were obtained in the presence of SCN, while the large polyatomic anion propionate, which is not conducted through CFTR, generated small, but significant $I_{para}$ (0.0 versus 0.13). $I_{para}$ is probably due to anion conductive pathways, including the paracellular path, that lie parallel to CFTR.

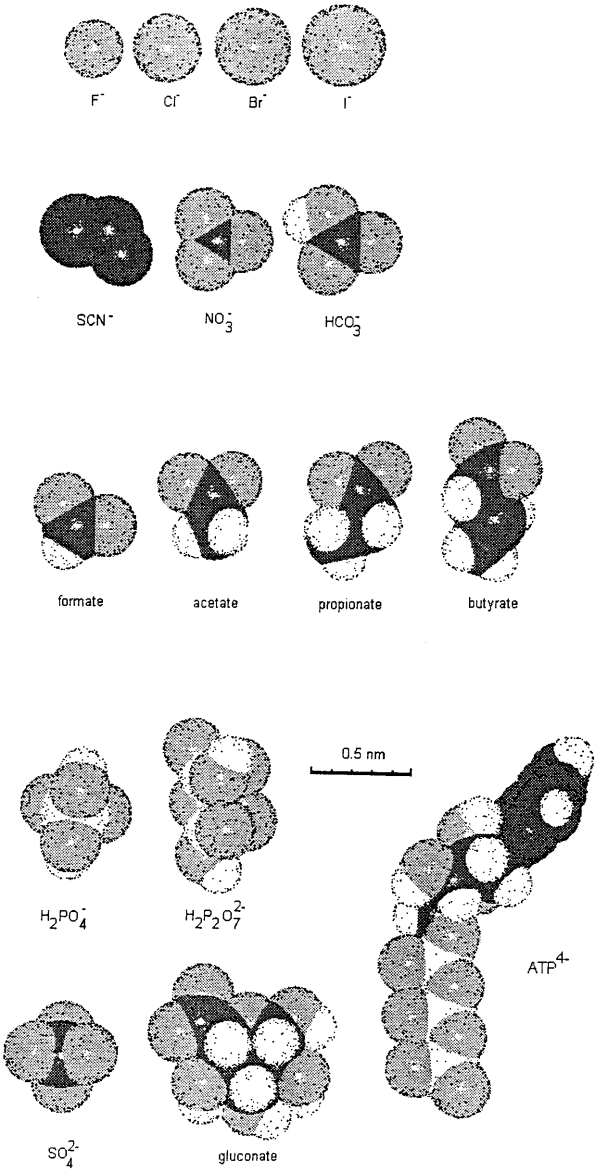


**Fig. 6A–E** Space-filling models of unhydrated test anions. **A** Halides. Diameters were (in nm): F=0.29, Cl=0.35, Br=0.39, I=0.42. Polyatomic anions are shown with medium and longest length. **B** SCN, $NO_3$ and $HCO_3$. Estimated medium length (in nm): SCN=0.42, $NO_3$=0.47 and $HCO_3$=0.52. Estimated long length (in nm): SCN=0.62, $NO_3$=0.52, and $HCO_3$=0.61. **C** Short-chain fatty acids. Estimated medium length (in nm) were very similar: formate=0.50, acetate=0.53, propionate=0.56, butyrate=0.55, whereas the longest lengths (in nm) were 0.59, 0.64, 0.74, and 0.82, respectively. **D** $PO_4$, PPi and ATP. Medium length (in nm): $PO_4$=0.56, PPi=0.56 and ATP=0.97. Longest lengths (in nm) were 0.59, 0.80, and 1.48, respectively. **E** $SO_4$ and Gluc. Estimated medium lengths (in nm): $SO_4$=0.53, gluconate=0.83. Estimated longest lengths (in nm) were 0.59 and 1.04, respectively

### The cut-off size for cAMP-stimulated anion permeation

In order to estimate CFTR's pore size, we estimated the effective unhydrated diameters for all anions. We assumed that these anions permeate lengthwise and are restricted by their width, so the largest width rectangular to

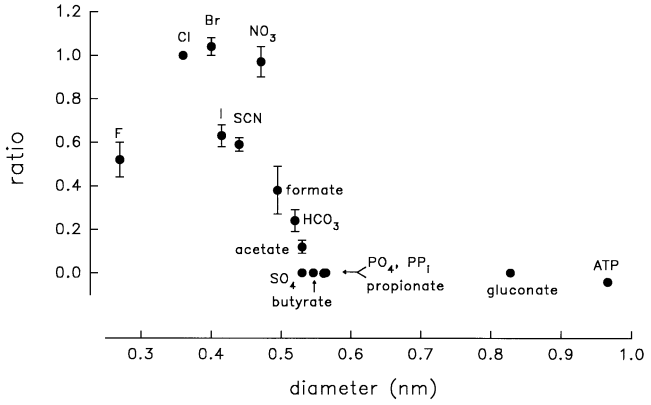


**Fig. 7** Plot of relative current ratios (corrected ratios, obtained from Table 1) versus the diameter of unhydrated anions. Polyatomic anions were modeled as rectangular prisms using a computer program that approximates ionic diameters in a three-dimensional configuration yielding estimates for the short, medium and longest coordinates of the molecules, as shown in Fig. 6. The diameters of molecules plotted here are equal to the medium lengths. Anions up to a diameter of 0.42 nm (the diameter of I) were well conducted. There were small, but detectable conductances for $HCO_3$ and acetate. No conductance changes were measured with anions >0.53 nm ($SO_4$, propionate, butyrate, $PO_4$, PPi, and ATP). This plot also illustrates that for ions with diameters <0.50 nm conductance does not correlate with size. Data are shown as means ±SE

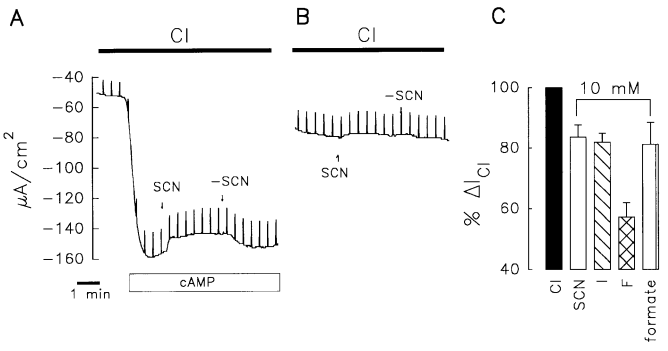


**Fig. 8A–C** Effect of SCN on CFTR-mediated Cl permeation. **A** Apical Cl currents are stimulated by cAMP. Further addition of 10 mM SCN to the mucosal Cl-containing solution reversibly blocks Cl currents. **B** Similar effects are measured in the presence of 10 mM I, F and formate. On average, apical Cl currents were blocked by 12.5%, 18.7%, 42.9% and 19.1% in the presence of 10 mM SCN, 10 mM I, 10 mM F and 10 mM formate, respectively. **C** Unstimulated parallel Cl currents were not affected by the addition of 10 mM SCN

the longest dimension of polyatomic anions was used as the effective diameter. Figure 6 shows space-filling models of all tested anions (unhydrated) to illustrate their sizes and shapes. Corrected current ratios from Table 1 were then plotted versus the effective diameter (Fig. 7). The sizes of the ions calculated here are very similar to those recently calculated by Lindsell et al. [17] using a different molecular modeling program. This plot yields a sharp decline of conductivity for ions larger than $NO_3$ (0.47 nm), and an exclusion of anions larger than acetate (0.53 nm). Although the conductance of ions does not necessarily correlate with size [37], the observed relationship between current and ionic size suggests a limiting smallest pore diameter of ≅0.53 nm that restricts current flow of larger ions. This correlates well with the apparent pore size of CFTR expressed exogenously in fibroblasts [17].

### Block of CFTR-mediated Cl currents by external I, F, SCN, and formate

We measured transient changes in cAMP-stimulated currents during exposure to solutions containing I, F, SCN, and formate (Figs. 1A, 2C and 4A), suggesting that these anions exerted transient inhibitory interactions on anion permeation. Since SCN (10 mM) has been shown to inhibit Cl transport in dog tracheal epithelium [36] and low concentrations (up to 10 mM) of I and SCN both permeate and block CFTR expressed in CHO cells [16, 32], it seems likely that similar effects occur for I, F, SCN, and formate during the interaction of these ions with CFTR in Calu-3 cells. We addressed this possibility by testing the effect of mucosal addition of 10 mM SCN on cAMP-stimulated Cl currents (Fig. 8A). Addition of 10 mM SCN, 10 mM I, 10 mM F or 10 mM formate to the apical solution effectively inhibited cAMP-stimulated Cl currents on average by 12.5±0.9% ($n$=4) for SCN, 18.7±3.7% ($n$=4) for I, 42.9%±6.0% ($n$=4) for F, and 11.6% and 26.6% ($n$=2) for formate. No effects were seen in unstimulated monolayers (shown for SCN in Fig. 8C), indicating that unstimulated currents permeate through a pathway that is different from the cAMP-stimulated pathway (probably CFTR).

## Discussion

Since the activity of CFTR might have depended on its protein and lipid environment and because many selectivity studies using patch-clamp techniques were performed at room temperature [7, 8, 17, 32] or 30–35°C [1], we investigated its conductivity selectivity in the apical membrane of an airway epithelial cell at 37°C. Our study allowed determination of the conductance properties of the apical plasma membrane (in the presence of cAMP) and also of parallel pathways (in the absence of cAMP). As discussed below, a comparison of our data for CFTR expressed in the apical membrane of Calu 3 tracheal cells to previous measurements of CFTR expressed endogenously in T84 cells and recombinantly in both frog oocytes and fibroblasts shows that:

1. CFTR has very similar anion conductance selectivity and apparent pore size no matter where it is expressed.
2. ATP, ADP and Pi are not conductive because they are too large to fit through CFTR's pore (0.53 nm diameter).
3. A variety of physiologically relevant anions (in addition to I and SCN) may affect CFTR's conductance to Cl.

We also found that the conductance in parallel to CFTR (probably tight junctions) exhibits a distinct conductance selectivity to anions that may be physiologically relevant in some circumstances.

CFTR expressed in the apical membrane of polarized Calu-3 airway cells has the following steady-state conductance selectivity for halides: Br (1.04)≥Cl(1.0)>I (0.59)≥F (0.52). The steady-state conductance of CFTR to the halides has been debated. The conductance selectivity of CFTR expressed in frog oocytes is Cl (1.0) >Br (0.6–0.65)>I (0.2–0.45) [12, 18]. In contrast, the conductance selectivity of apical CFTR in T84 cells is Cl (1.0) >Br(0.9)>I (0.5) [1], which was similar to the selectivity determined by patch-clamp measurements of CFTR conductance expressed in 3T3 [1] or HeLa [1] cells [Br (1.0–1.3)≥Cl (1.0)>I (0.3–0.4)]. The main differences among these are that the Br/Cl selectivity is lower for CFTR in frog oocytes (Br/Cl=0.6–0.65; [12, 18]) than in Calu 3 (Br/Cl=1.04), T84 (Br/Cl=0.9; [1]), HeLa (Br/Cl=1.0; [1]) and 3T3 (Br/Cl=1.3; [1]) cells. The similar conductances of Br and Cl combined with subtle methodological differences may have led to the inversions of this pair in the different laboratories. We conclude that native human CFTR in the apical membrane of Calu 3 cells has a similar steady-state conductance selectivity to halides (Br≥Cl>I>F) as CFTR expressed in both polarized colonic cells and nonpolar fibroblasts.

A similar conclusion can now be extended to CFTR's selectivity for polyatomic anions. Apical CFTR conductance in Calu-3 cells showed the sequence Cl (1.0)≥$NO_3$ (0.97)>formate (0.38)>$HCO_3$ (0.24)>acetate (0.12), which is similar to the conductance sequence for CFTR expressed in frog oocytes [18]: Cl (1.0)>$NO_3$ (0.8)>formate (0.5). We note, however, that the SCN/Cl conductance selectivity is lower for CFTR in frog oocytes (SCN/Cl =0.14; [12, 18]) than in Calu 3 (SCN/Cl=0.6) or CHO (SCN/Cl=1.2; [17]) cells. The apparent discrepancies with SCN may have resulted from the unique properties of this high-permeability, low-conductance ion. Mansoura et al. [18] have found, for CFTR expressed in frog oocytes, that the SCN permeability is larger than that for Cl ($P_{SCN}/P_{Cl}$=3.4), while SCN conductance was smaller than that for Cl ($G_{SCN}/G_{Cl}$=0.14). Similar effects were observed [18] with $NO_3$ ($P_{NO3}/P_{Cl}$=1.4 and $G_{NO3}/G_{Cl}$=0.8). These differences between permeability and conductance selectivities appear to be due to the fact that these ions have a high affinity for sites within the pore (and therefore high permeability), but the high affinity leads to tight binding (and therefore to low conductance) (see [17, 18, 34]).

Our data indicate that ionic size does not play a major role in determining the steady-state conductance of CFTR to ions that are smaller than CFTR's cut-off size. This probably results from the fact that the energies of interaction of ions with water (hydration) and with sites within the pore are both important for permeant ions (see [6, 37]; also [33, 34]). Ionic size becomes important when the channel and the ion are approximately the same dimension: there is a steep dependence for CFTR's conductance ($\Delta I_X/\Delta I_{Cl}$) on ionic size for anions larger than $NO_3$ (0.47 nm), leading to zero conductance for ions larger than acetate (0.53 nm) (Fig. 7). These data suggest that the pore size of apical CFTR in Calu 3 cells restricts ions whose diameters are greater than 0.47 nm, and excludes all anions larger than 0.53 nm. This is illustrated by the singly charged SCFA, whose effective diameters ranged from 0.49 nm to 0.56 nm. Formate (0.49 nm) and acetate (0.53 nm) were conducted while propionate (0.56 nm) and butyrate (0.55 nm) were not.

Therefore, it seems that the polyvalents $PO_4$, PPi and ATP cannot permeate because of their large size. It is unlikely that differences in the charge of these anions accounts for this result because $PO_4$, 53% of which occurs in its monovalent form at a pH of 7.4, was not conducted. Thus, consistent with previous measurements made by Reddy et al. [24], neither CFTR (see [25, 26]) nor associated conductances in the apical membrane [20] of Calu 3 cells conduct ATP. $SO_4$ may not have been conducted because it is both large (0.53 nm) and bivalent; therefore, it may have been bound strongly within the channel. CFTR's effective pore diameter of ≅0.53 nm in Calu 3 cells is nearly the same as its estimated value in CHO cells (0.53–0.55 nm) [9, 17, 31]. Other Cl channels seem to have similar pore sizes, e.g., the outwardly rectifying Cl channel (0.55 nm) [10], the glycine receptor (0.52 nm) and γ-aminobutyric acid receptor (0.56 nm) [3].

The small, but significant conductances to the small, physiologically relevant anions $HCO_3$, formate and acetate (Table 2 and Fig. 4; also see [7, 8, 13, 14, 17, 19, 21, 35]) could result in secretion or absorption across epithelial cells depending on the total transmembrane electrochemical gradients for these ions. Whether CFTR contributes physiologically to the transport of these ions across cells of the bile and pancreatic ducts and the small and large intestine will need to be investigated using intact epithelial sheets or similar preparations (e.g., [13]). Some CF mutations are associated with altered single-channel properties [18, 28] and altered halide selectivity, e.g., Br>Cl=I [29] or Br>I>Cl>F [1]. Whether CF-associated mutations in the pore region(s) of CFTR [29] affect the selectivity of physiologically relevant anions that are conducted through CFTR (i.e., $HCO_3$) remains to be determined.

The tight binding of SCN within the pore probably enables this highly permeant ion to block CFTR at concentrations up to 10 mM [12, 16, 18, 32]. SCN has also been shown recently to block the steady-state conductance of CFTR [33]. Data from the present study extend these findings by showing that, in addition to SCN and I, both F and formate also inhibit the Cl conductance through CFTR in the apical membrane of Calu 3 cells. Similarly, preliminary work (B. Illek and T.E. Machen) has shown that 10 mM $HCO_3$ inhibits Cl conductance through CFTR. Therefore, Cl permeation across CFTR is probably affected by the presence of physiologically rel-

evant anions such as formate, acetate and $HCO_3$. The effects of $HCO_3$ on Cl permeation are the subject of an ongoing investigation.

Our measurements also yielded information about the anion conductivity through pathways lying parallel CFTR. As seen from the summary data in Fig. 5, the magnitude of baseline currents for halides (i.e., $I_{ctrl}$, due to conductance through parallel pathways) was smaller by an average factor of 2 compared to that exhibited by CFTR (i.e., $\Delta I$). The parallel permeability pathway exhibited a different sequence for SCN (SCN=Cl) and exhibited a significant conductance for the relatively large anion propionate. These results and previous experiments showing that the CFTR blocker DPC has no effect on $I_{ctrl}$ [14] indicate that $I_{ctrl}$ is not due to permeation of CFTR, but is more likely attributable to permeation of anions through parallel pathways (e.g., tight junctions). The paracellular pathway appears to have selective conductance properties that are similar to, but distinct from, CFTR. The tight junctions could therefore play a role in the transepithelial transport of specific anions under proper physiological conditions.

**Acknowledgments** This work was funded by grants from the National Institutes of Health (DK 57199), the Cystic Fibrosis Foundation (Illek96F0), and the Deutsche Forschungsgemeinschaft (Il28/2–3). A. Tam was a recipient of a Student Traineeship from the Cystic Fibrosis Foundation.

## References

1. Anderson MP, Gregory RJ, Thompson S, Souza DW, Paul S, Mulligan RC, Smith AE, Welsh MJ (1991) Demonstration that CFTR is a chloride channel by alteration of its anion selectivity. Science 253:202–205
2. Bell CL, Quinton PM (1992) T84 cells: anion selectivity demonstrates expression of Cl conductance affected in cystic fibrosis. Am J Physiol 262:C555–C562
3. Borman J, Hamill OP, Sakmann B (1987) Mechanism of anion permeation through channels gated by glycine and gamma-aminobutyric acid in mouse cultured spinal neurones. J Physiol (Lond) 385:243–286
4. Cliff WH, Frizzell RA (1990) Separate $Cl^-$ conductances activated by cAMP and $Ca^{2+}$ in $Cl^-$-secreting epithelial cells. Proc Natl Acad Sci USA 87:4956–4960
5. Cliff WH, Schoumacher RA, Frizzell RA (1992) cAMP-activated Cl channels in CFTR-transfected cystic fibrosis pancreatic epithelial cells. Am J Physiol 262:C1154–C1160
6. Eisenman G, Horn R (1983) Ionic selectivity revisited: the role of kinetic and equilibrium processes in ion permeation through channels. J Membr Biol 76:197–225
7. Gray MA, Pollard CE, Harris A, Coleman L, Greenwell JR, Argent BE (1990) Anion selectivity and block of the small-conductance chloride channel on pancreatic duct cells. Am J Physiol 259:C752–C761
8. Gray MA, Plant S, Argent BE (1993) cAMP-regulated whole cell chloride currents in pancreatic duct cells. Am J Physiol 264:C591–C602
9. Grygorczyk R, Tabcharani JA, Hanrahan JW (1996) CFTR channels expressed in CHO cells do not have detectable ATP conductance. Am J Physiol 272:C1058–C1066
10. Halm DR, Frizzell RA (1992) Anion permeation in an apical membrane chloride channel of a secretory epithelial cell. J Gen Physiol 99:339–366
11. Haws C, Finkbeiner WE, Widdicombe JH, Wine JJ (1994) CFTR in Calu-3 human airway cells: channel properties and role in cAMP-activated Cl conductance. Am J Physiol 266: L692–L707
12. Hipper A, Mall M, Greger R, Kunzelmann K (1995) Mutations in the putative pore-forming domain of CFTR do not change anion selectivity of the cAMP-activated Cl conductance. FEBS Lett 374:312–316
13. Hogan DL, Crombie DL, Isenberg JI, Svendsen P, Schaffalitzky de Muckadell OB, Ainsworth MA (1997) CFTR mediates cAMP- and $Ca^{2+}$-activated duodenal epithelial HCO3 secretion. Am J Physiol 262:G872–G878
14. Illek B, Yankaskas JR, Machen TE (1997) cAMP and genistein stimulate $HCO_3$ conductance through CFTR in human airway epithelia. Am J Physiol 272:L752–L761
15. Li C, Ramjeesingh M, Bear CE (1996) Purified cystic fibrosis transmembrane conductance regulator (CFTR) does not function as an ATP channel. J Biol Chem 271:11623–11626
16. Linsdell P, Tabcharani JA, Hanrahan JW (1997) Multi-ion mechanism for ion permeation and block in the cystic fibrosis transmembrane conductance regulator chloride channel. J Gen Physiol 110:365–377
17. Linsdell P, Tabcharani JA, Rommens JM, Hou YX, Chang XB, Tsui LC, Riordan JR, Hanrahan JW (1997) Permeability of wild-type and mutant cystic fibrosis transmembrane conductance regulator chloride channel to polyatomic anions. J Gen Physiol 110:355–364
18. Mansoura MK, Smith SS, Choi AD, Richards NW, Strong TV, Drumm ML, Collins FS, Dawson DC (1998) Cystic fibrosis transmembrane conductance regulator (CFTR). Anion binding as a probe of the pore. Biophys J 74:1320–1332
19. Ohrui T, Skach W, Thompson M, Matsumoto-Pon J, Calayag C, Widdicombe JH (1994) Radiotracer studies of cystic fibrosis transmembrane conductance regulator expressed in *Xenopus* oocytes. Am J Physiol 266:C1586–C1593
20. Pasyk EA, Foskett JK (1997) Cystic fibrosis transmembrane conductance regulator-associated ATP and adenosine 3′-phosphate 5′-phosphosulfate channels in endoplasmic reticulum and plasma membranes. J Biol Chem 272:7746–7751
21. Poulsen JH, Fischer H, Illek B, Machen TE (1994) Bicarbonate conductance and pH regulatory capability of cystic fibrosis transmembrane conductance regulator. Proc Natl Acad Sci USA 91:5340–5344
22. Quinton PM (1990) Cystic fibrosis: a disease in electrolyte transport. FASEB J 4:2709–2717
23. Quinton PM, Reddy MM (1989) Cl conductance and acid secretion in the human sweat duct. Ann NY Acad Sci 574: 438–446
24. Reddy MM, Quinton PM, Haws C, Wine JJ, Grygorczyk R, Tabcharani JA, Hanrahan JW, Gunderson KL, Kopito RR (1996) Failure of the cystic fibrosis transmembrane conductance regulator to conduct ATP. Science 271:1876–1879
25. Reisin IL, Prat AG, Abraham EH, Amara JF, Gregory RJ, Ausiello DA, Cantiello HF (1994) The cystic fibrosis transmembrane conductance regulator is a dual ATP and chloride channel. J Biol Chem 269:20584–20591
26. Schwiebert EM, Egan ME, Hwang FH, Fulmer SB, Allen SA, Cutting GR, Guggino WB (1995) CFTR regulates outwardly rectifying chloride channels through an autocrine mechanism involving ATP. Cell 81:1063–1073
27. Shen BQ, Finkbeiner WE, Wine JJ, Mrsny RJ, Widdicombe JH (1994) Calu-3: a human airway epithelial cell line that shows cAMP-dependent Cl secretion. Am J Physiol 266: L493–L501
28. Sheppard DN, Rich DP, Ostedgaard LS, Gregory RJ, Smith AE, Welsh MJ (1993) Mutations in CFTR associated with mild-disease form Cl- channels with altered pore properties. Nature 362:160–164
29. Sheppard DN, Travis SM, Ishihara H, Welsh MJ (1996) Contribution of proline residues in the membrane-spanning domains of cystic fibrosis transmembrane conductance regulator

to chloride channel function. J Biol Chem 271:14995–15001
30. Song L, Hobaugh MR, Shustak C, Cheley S, Bayley H, Gouaux JE (1996) Structure of *Staphylococcal* α-hemolysin, a heptameric transmembrane pore. Science 274:1859–1866
31. Tabcharani JA, Hanrahan JW (1993) Permeation in the cystic fibrosis transmembrane conductance regulator (CFTR) chloride channel (abstract). Biophys J 64:A17
32. Tabcharani JA, Rommens JM, Hou YX, Chang XB, Tsui LC, Riordan JR, Hanrahan JW (1993) Multi-ion pore behavior in the CFTR chloride channel. Nature 366:79–82
33. Tabcharani JA, Linsdell P, Hanrahan JW (1997) Halide permeation in wild-type and mutant cystic fibrosis transmembrane conductance regulator chloride channels. J Gen Physiol 110: 341–354
34. Tsien RW, Hess P, McCleskey EW, Rosenberg RL (1987) Calcium channels: mechanisms of selectivity, permeation and block. Annu Rev Biophys Biol Chem 16:262–290
35. Von Engelhardt W, Rechkemmer G (1992) Segmental differences of short-chain fatty acid transport across guinea pig large intestine. Exp Physiol 77:491–509
36. Widdicombe JH, Welsh MJ (1980) Anion selectivity of the chloride-transport process in dog tracheal epithelium. Am J Physiol 239:C112–C117
37. Wright EM, Diamond JM (1977) Anion selectivity in biological systems. Physiol Rev 57:109–156